Plasmonically Enhanced Optical Accelerator for Nonlinear Signal Processing Based on Artificial Neural Networks

Tobias Blatter(1,*), Amane Zürrer(1), Yannik Horst(1), Christos Pappas(2), George Giamougiannis(2), Apostolos Tsakyridis(2), Manuel Kohli(1), Ueli Koch(1), Miltiadis Moralis-Pegios(2), Nikos Pleros(2) and Juerg Leuthold(1,*)
[1]*ETH Zurich, Institute of Electromagnetic Fields (IEF), 8092 Zurich, Switzerland*
[2]*Department of Informatics, Aristotle University of Thessaloniki, 54124, Thessaloniki*
**Tobias.Blatter@ief.ee.ethz.ch, Juerg.Leuthold@ief.ee.ethz.ch*

Abstract: We reconstruct a 48 Gbit/s nonlinearly distorted optical signal using an artificial neural network (ANN). The digital ANN execution exceeds traditional nonlinear equalizers, while its analog acceleration using plasmonic-organic-hybrid modulators surpasses conventional digital linear equalizers. © 2024 The Author(s)

1. Introduction

The current mitigation strategies for linear and nonlinear distortions in optical fiber communication links predominantly rely on digital hardware. To cope with increasing data speeds, high-speed electronics are required, which results in increasing costs and power demands. Traditional algorithms, based on Volterra series and digital backpropagation algorithms, are now being re-evaluated in light of these aspects. Recent studies have indicated that artificial neural networks (ANNs) can significantly trim down computational power requirements [1].

Executing multiplication and accumulation (MAC) operations on photonic platforms promises not just computational acceleration but also a significant reduction in power consumption [2, 3]. Combining the advantages of ANNs with the advantages of photonic computing will even further decrease the power consumption and increase the computational speed. The most organic way to address these challenges is by performing signal processing directly on the analog optical signal. Recently, this approach has been successfully demonstrated by processing 16 Gbit/s [4] and 40 Gbit/s [5] optical signals with photonic perceptrons.

In this work, we harness for the first time the characteristics of plasmonic-organic-hybrid Mach-Zehnder modulators (MZMs) in a photonic accelerator. MZMs map the electrical signal into the optical domain, where the MAC operations are executed. Recognized for their large bandwidths reaching up to 500 GHz, atto-joule energy consumption per bit, and compact footprints [6, 7], plasmonic MZMs present a promising way to further increase the computational speed compared to their photonic counterpart [8]. On our chip, the MAC operation of an ANN that counteracts the nonlinear effects of a driver amplifier is executed analog on an integrated photonic chip. Notably, the analog-processed signal with a line rate of 48 Gbit/s surpasses the digital linear filter in terms of signal-to-noise ratio (SNR). Furthermore, its digital counterpart outperformed standard nonlinear filters while keeping the computational demands low.

2. Device Concept and Experimental Setup

We acquired the training data for the digital ANN using a standard intensity modulation and direct detection (IM/DD) setup as shown in Fig. 1(a). The transmitted bits were randomly generated, in order to avoid overfitting that may occur with pseudo-random bit streams [9]. The nonlinearities arose from the electrical amplifier that drove a commercial MZM with a 30 GHz 3 dB-bandwidth. The ANN training used 10% of the symbols from the sampled and timing-recovered signal, denoted as s_{Rx}. The ANN's input layer processes four time-delayed symbols with a two-fold oversampling. The hidden layer has four neurons, each with a sigmoid activation function. In contrast, the output layer consists of a single neuron with a linear activation function. The ANN's training objective was to ensure that its output mirrors the transmitted symbol, see Fig. 1(b).

In the optical ANN (OANN) evaluation, see Fig. 1(c), the hidden layer's output was computed offline using the recorded data s_{Rx}. These four resulting signals were then relayed to the plasmonic MZM, which maps them to the optical intensity of a carrier at frequency f_i. The index i indicates the i-th laser. The weighting process is facilitated by a thermo-optical (T/O) MZM placed before the plasmonic MZM. A microscope image of the chip is shown as inset in Fig. 1(c). Post-chip signals sharing weight signs, represented by s_+ and s_- are combined, amplified, and directed to two photodiodes (PD). Due to the significant gap between the frequencies f_i compared to the PD's bandwidth, the PD captures the weighted sum of the signals. After recording with a digital sampling oscilloscope, the two signals are subtracted from each other and the linear activation function, including the biases, is applied. An additive white

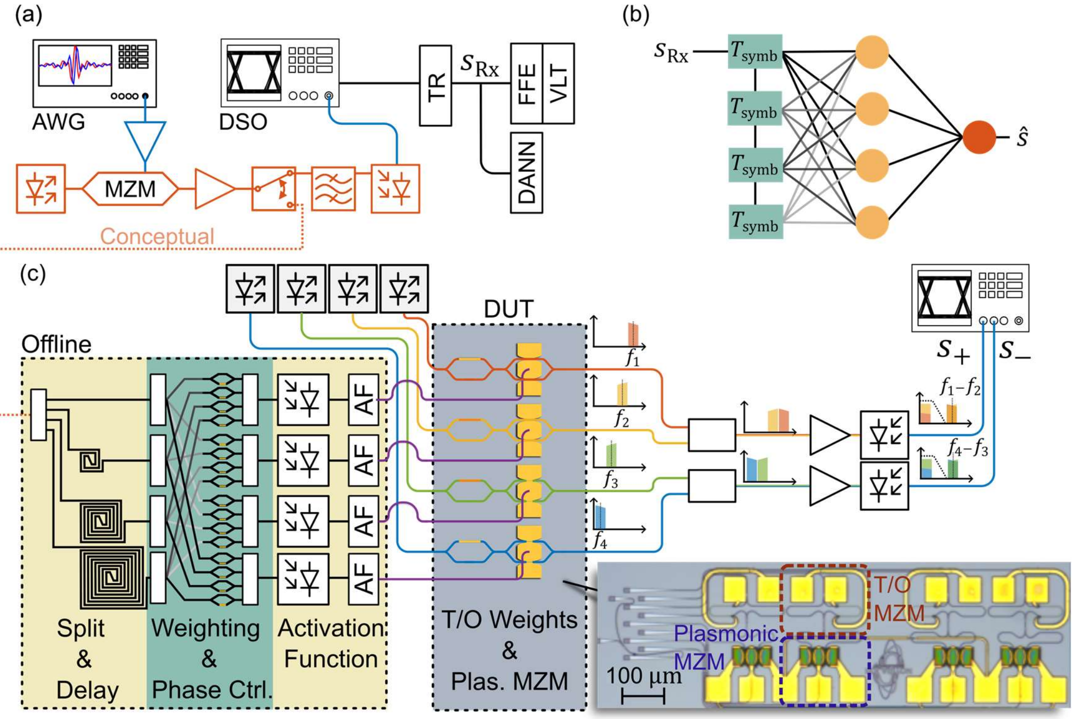

Fig. 1. (a) Schematic representation of the signal (s_{Rx}) acquisition. After timing recovery (TR), 10% of the symbols are used to train the ANN. 90% of the symbols are used to test the ANN both, digitally and optically. As a baseline, the SNR is estimated after TR, linear filter (FEE) and Volterra series. (b) Schematic of the ANN. As an input, it takes four symbols with an oversampling of two. (c) Analog ANN concept: The optical signal after the channel directly enters an on-chip split and delay section. Subsequently, the signal undergoes weighting and phase adjustments to be acquired in a PD. An activation function (AF) is then applied on the electrical signal. Experimentally, the outcomes were computed offline using the s_{Rx} data. The resultant signals drive the four plasmonic MZMs, modulating the carrier's intensity. Weight application is handled by the T/O MZM. After merging, the weighted sum is captured. The weight's sign is retained by separately documenting the sum corresponding to that weight, i.e., s_+ and s_-. The difference between and s_+ and s_- was calculated offline and correspond to the ANN's output $\hat{s}$. The inset provides a microscopic view on the chip.

Gaussian noise (AWGN) channel is fitted to the resulting signal in order to quantify the performance of the ANN by the SNR.

As a baseline for comparison, the pre-recorded signal s_{Rx} was further propagated through a digital signal processing chain. This included timing recovery (TR), a T/2-spaced feed-forward equalizer (FFE), and a Volterra equalizer. To further compare the performance, we also executed the ANN digitally (DANN) by processing s_{Rx}, see Fig. 1(a). At each step, an AWGN channel was fitted to the signal. The resulting SNR estimation is used to compare the performance.

3. Experimental Results

Our results demonstrate that the DANN outperforms both the (digital) FFE and the Volterra equalizers in terms of SNR. Moreover, the OANN outperforms the FFE in SNR metrics. The signal being processed had a rate of 16 GBd and utilized an 8-PAM modulation format, effectively achieving a 48 Gbit/s data rate.

In Fig. 2(a), the SNR values after the TR, FEE and Volterra are depicted in red, yellow, and green bars, respectively. The light blue bar shows the SNR after the DANN processes the TR signal. To elaborate, the SNR after TR, FEE, and Volterra read 12.6, 15.4, and 21.4 dB, respectively. Meanwhile, the SNR after the DANN reads 23.4 dB, corresponding to a gain of 2 dB compared to the Volterra equalizer.

In terms of their configuration, the FEE employed 151 taps, while the Volterra equalizer used 151, 11, 51 taps for its first, second and third order, respectively. In contrast, the ANN only used 8 taps at its input, 4 neurons in the middle layer and a single linear neuron at its output layer. Our findings indicate that in the context of our studied case, the ANN does not only surpass FEE and Volterra in performance, but also with reduced computational demands.

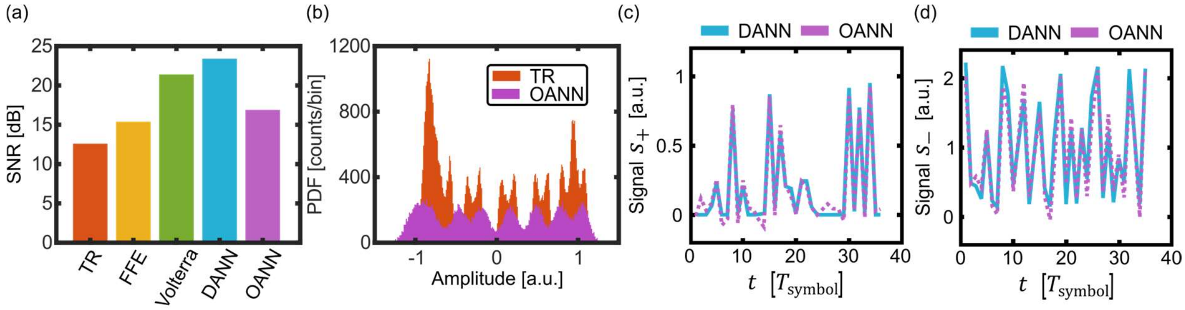

Fig. 2. (a) Comparison of SNR values after processing through TR, FEE, Volterra, and DANN with the TR signal achieving an SNR of 12.6 dB, FEE with 15.4 dB, Volterra with 21.4 dB, and DANN showing a notable increase to 23.4 dB. The application of DANN on a plasmonic-enhanced optical accelerator results in an SNR of 16.9 dB. (b) Histogram of the recoded TR and OANN signal. (c) and (d) Signal traces for s_+ and s_-, respectively, with the expected DANN trace in blue and the recorded ANN trace in pink.

Further investigations were conducted by executing the ANN on the plasmonic-enhanced optical accelerator, referred as OANN. As shown by the blue bar in Fig. 2(a), the signal after the OANN had an SNR value of 16.9 dB. This represents a decrease of 4.5 dB when compared to the DANN, but it still manages to outperform the digital FEE by 1.6 dB. The bit-error rate decreased from $8.0 \cdot 10^{-2}$ after the FEE to $3.8 \cdot 10^{-2}$ with the OANN, which is below the SD-FEC limit.

In Fig. 2(b), the histogram displays the distribution of the recorded TR and OANN signal. The TR signal is represented by the red bins. Notably, 5 out of the 8 levels are distinctly separated, while the outer symbols appear compressed. The OANN, depicted in pink, effectively mitigates this compression.

Focusing on Fig. 2(c) and (d), we plotted the traces for signals s_+ and s_-. The expected DANN trace is colored in blue, whereas the recorded OANN trace is shown in pink. Quantitatively, the root mean squared errors amounted to 0.119 for s_+ and 0.09 for s_-.

4. Conclusion

Our study marks the first utilization of plasmonic MZMs for directly processing analog optical signals. The bandwidth, power consumption, and compact nature of plasmonic MZMs make them a preferable alternative to their photonic counterparts. Through our investigations, we have observed that the signal processing using an ANN outperforms traditional equalizers like FEE and Volterra, both in terms of SNR and computational requirements. Furthermore, when executed on a plasmonically enhanced optical accelerator, the ANN, although slightly reduced in performance compared to its pure digital counterpart, still surpasses the digital FEE.

5. Acknowledgements

We thank the Horizon 2020 projects PlasmoniAC (871391) and NEBULA (871658), and Polariton Technologies for providing the plasmonic MZM. Polariton Technologies thanks NLM Photonics for the organic electro-optical material and the Cleanroom and Operations team of the Binning and Rohrer Nanotechnology Center (BRNC) for their support.

6. References

[1] B. I. Bitachon *et al.*, "Deep learning based digital backpropagation demonstrating SNR gain at low complexity in a 1200 km transmission link," Optics Express, vol. 28, no. 20, pp. 29318-29334, 2020.
[2] A. H. Atabaki *et al.*, "Integrating photonics with silicon nanoelectronics for the next generation of systems on a chip," Nature, vol. 556, no. 7701, pp. 349-354, 2018.
[3] B. J. Shastri *et al.*, "Photonics for artificial intelligence and neuromorphic computing," Nat. Photonics, vol. 15, no. 2, pp. 102-114, 2021.
[4] M. Mancinelli *et al.*, "A photonic complex perceptron for ultrafast data processing," Sci. Rep., vol. 12, no. 1, pp. 4216, 2022.
[5] E. Staffoli *et al.*, "Recovery of 40 Gbps PAM4 in a 50 km optical link through a delayed complex perceptron," in *SiPhotonics*, 2023, pp. 1-2
[6] M. Burla *et al.*, "500 GHz plasmonic Mach-Zehnder modulator enabling sub-THz microwave photonics," APL Photonics, vol. 4, no. 5, pp. 056106, 2019.
[7] W. Heni *et al.*, "Plasmonic IQ modulators with attojoule per bit electrical energy consumption," Nat. Commun., vol. 10, no. 1, pp. 1694, 2019.
[8] A. R. Totović *et al.*, "Femtojoule per MAC Neuromorphic Photonics: An Energy and Technology Roadmap," IEEE J Sel Top Quantum Electron, vol. 26, no. 5, pp. 1-15, 2020.
[9] T. A. Eriksson *et al.*, "Applying Neural Networks in Optical Communication Systems: Possible Pitfalls," IEEE Photonics Technol. Lett., vol. 29, no. 23, pp. 2091-2094, 2017.